Assessing the Antiproliferative Potential of a Novel Combretastatin A4 Derivative via Modulating Apoptosis, MAPK/ERK and PI3K/AKT Pathways in Human Breast Cancer Cells

Maiiada Nazmy, Dalia Abu-Baih, Mahmoud Elrehany, Muhamad Mustafa, Omar Aly, Azza El-Sheikh, Moustafa Fathy

Frontiers in Bioscience Landmark

Front. Biosci. (Landmark Ed) **2023**; 28(8): 185
https://doi.org/10.31083/j.fbl2808185

Original Research

Assessing the Antiproliferative Potential of a Novel Combretastatin A4 Derivative *via* Modulating Apoptosis, MAPK/ERK and PI3K/AKT Pathways in Human Breast Cancer Cells

Maiiada H. Nazmy[1,†], Dalia H. Abu-baih[2,†], Mahmoud A. Elrehany[2], Muhamad Mustafa[3,4], Omar M. Aly[5], Azza A. K. El-Sheikh[6], Moustafa Fathy[1,7,*]

[1]Department of Biochemistry, Faculty of Pharmacy, Minia University, 61519 Minia, Egypt
[2]Department of Biochemistry and Molecular Biology, Faculty of Pharmacy, Deraya University, 61111 Minia, Egypt
[3]Department of Medicinal Chemistry, Faculty of Pharmacy, Deraya University, 61111 Minia, Egypt
[4]IBMM, CNRS, ENSCM, Université de Montpellier, 34095 Montpellier, France
[5]Medicinal Chemistry Department, Faculty of Pharmacy, Port said University, 42526 Port said, Egypt
[6]Basic Health Sciences Department, College of Medicine, Princess Nourah bint Abdulrahman University, 11671 Riyadh, Saudi Arabia
[7]Department of Regenerative Medicine, Graduate School of Medicine and Pharmaceutical Sciences, University of Toyama, 930-0194 Toyama, Japan
*Correspondence: mostafa_fathe@minia.edu.eg (Moustafa Fathy)
[†]These authors contributed equally.

Academic Editor: Rumiana Tzoneva
Submitted: 29 April 2023 Revised: 29 May 2023 Accepted: 25 June 2023 Published: 28 August 2023

Abstract

Background: Breast cancer is the most predominant tumor in women. Even though current medications for distinct breast cancer subtypes are available, the non-specificity of chemotherapeutics and chemoresistance imposes major obstacles in breast cancer treatment. Although combretastatin A-4 (CA-4) has been well-reported to have potential anticancer activity, *in vivo* studies of CA-4 reveal a decrease in its activity. In this respect, a series of CA-4 analogues have been designed, from which one analog [(1-(3-chloro-4-fluorophenyl)-N-(2methoxyphenyl)-5-(3,4,5-trimethoxyphenyl)-1H-1,2,4-triazole-3-carboxamide, $C_{25}H_{22}ClFN_4O_5$] showed drastic cytotoxicity against breast cancer cells. Therefore, this research focused on investigating the *in vitro* molecular mechanism underlying the cytotoxicity of the CA-4 analogue, particularly the MAPK/ERK as well as PI3K/AKT pathways as attractive therapeutic targets in breast cancer. **Methods**: The cell viability of MCF-7, MDA-MB231, and MDA-MB453 was assessed after treatment with the CA-4 analogue, and apoptosis was analyzed *via* Annexin V-FITC/PI dual staining. MAPK/ERK and PI3K/AKT were thoroughly assessed using western blotting. Real-time PCR was used to estimate apoptosis-related markers, including the *P53*, *Bcl-2-associated X protein* (*Bax*), and *B-cell lymphoma 2* (*Bcl2*) genes. **Results**: The CA-4 analogue reduced the survival of all cancerous cells in a concentration-dependent manner and induced apoptosis through the mitochondrial pathway (39.89 $\pm$ 1.5%, 32.82 $\pm$ 0.6%, and 23.77 $\pm$ 1.1% in MCF-7, MDA-MB231, and MDA-MB453 cells), respectively. The analogue also attenuated the expression of pMEK1/2/t-MEK1/2, p-ERK1/2/t-ERK1/2, p-PI3K/t-PI3K, and p-AKT/t-AKT proteins in all three cancer cell lines in a time-dependent manner. Furthermore, the CA-4 analogue upregulated the expression of the *P53* gene and dramatically increased the ratio of *Bax/Bcl2* genes. **Conclusions**: The enhanced cytotoxicity can be attributed to substituting the hydroxyl group in CA-4 with chlorine in the meta-position of ring B, substituting the para-methoxy group in CA-4 with fluorine in the analogue, and lastly, introducing an extension to the compound's structure (ring C). Therefore, CA-4 analogue can attenuate the proliferation of human breast cancer cells by inducing apoptosis and simultaneously suppressing the MAPK/ERK and PI3K/AKT pathways.

Keywords: breast cancer; combretastatin A-4; anticancer; MAPK/ERK; PI3K/AKT; apoptosis

1. Introduction

Breast cancer is among the most predominant tumors in females globally, with alarmingly increasing incidence rates. In 2020, more than 2.3 million women were newly diagnosed with breast cancer, and 680,000 reported death [1]. The intricate nature of breast cancer is largely attributed to the presence of malignant lesions in the ductal epithelium of the breast, creating a diverse array of distinct subtypes [2]. The literature extensively classifies various forms of breast cancer into distinct groups, based on the expression of key receptors such as the estrogen receptor (ER), progesterone receptor (PR), and human epithelial receptor 2 (HER2) [3]. Breast cancers can be hormonally dependent, HER2 positive, or triple-negative breast cancer (TNBC) [4]. Each of these subtypes has distinct risk factors, treatment responses, and genetic traits. The complexity and diversity of these subtypes underline the challenges involved in diagnosing and treating breast cancer [5,6].

In recent years, remarkable progress has been made in the field of cancer treatment, offering numerous options for those fighting breast cancer, depending on the kind and severity of the disease. Although this undoubtedly has led

to improved patient outcomes, the effectiveness of current treatments and patient compliance are severely hindered by high treatment costs, developed resistance, and off-target toxicity [7,8]. The presence of multi-drug resistance and the non-specificity of chemotherapeutics present major obstacles in cancer treatment [9–11]. In light of these limitations, there is a dire need to identify or develop innovative and effective modalities for breast cancer therapy [4].

The mitogen-activated protein kinase (MAPK) and phosphatidylinositol 3-kinase (PI3K)/protein kinase B (AKT) signaling pathways govern critical cellular events such as cell proliferation, regeneration, survival, and invasion, which play a key role in breast cancer progression [12]. Early research reveals that those pathways are constitutively active in breast tumors through various mechanisms [13]. Sustained activation of these pathways not only prevents breast cancer cell apoptosis but also contributes significantly to chemoresistance. In preclinical models, suppressing these pathways has been shown to increase the susceptibility of breast cancerous cells toward chemotherapeutics. However, manipulating only one of these pathways is insufficient for successful management of breast cancer [14]. Therefore, concurrent targeting of the PI3K/AKT and MAPK pathways might be a potential therapeutic approach for breast carcinoma.

Recently, there has been increased interest in screening new alternative activities for natural [15] or synthetic [16] candidates that modulate pathways involved in carcinogenesis [17]. Combretastatin A-4 (CA-4) is an alkaloid extracted from the willow tree, *Combretum caffrum*, which shows robust cytotoxicity against numerous human cancer cells. Its cytotoxic activity is attributed to the inhibition of tubulin polymerization by binding to the β-tubulin colchicine binding site [18–20]. However, *in vivo* studies have revealed a drastic decline in CA-4 activity due to isomerization of its cisoid configuration into the *trans* form. To address this issue, several research groups have introduced various heterocyclic rings (such as oxadiazoles, triazoles, imidazoles, and thiadiazoles) to restrict the rotation of the olefinic double bond [21]. The cytotoxic activity of these synthetic derivatives against breast cancer has been studied [22,23].

In a previous study, we synthesized a novel CA-4 analogue, (1-(3-chloro-4-fluorophenyl)-N-(2methoxyphenyl)-5-(3,4,5-trimethoxyphenyl)-1H-1,2,4-triazole-3-carboxamide, C25H22ClFN4O5, with a molecular weight of 512.92 Da), using 1,2,4-triazole to link ring-A (3,4,5-trimethoxy phenyl) and ring-B (3Cl-4-F-phenyl) [24] (Fig. 1). This study demonstrated that the CA-4 analogue exhibited potent antiproliferative activity against several human cancer cells, such as MCF-7 breast cancer, with enhanced activity and stability compared to CA-4. These results motivated us to further examine the cytotoxic activity of this novel analogue on different breast cancer subtypes (hormonally dependent, HER2+, and TNBC). Additionally, we aimed to illustrate the molecular mechanism beyond its anticancer potential against these breast carcinoma cell lines by investigating apoptosis, MAPK/ERK, and PI3K/AKT pathways.

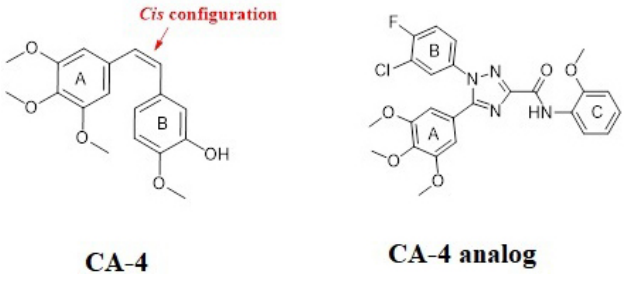

Fig. 1. Chemical structure of combretastatin A-4 (CA-4) and its analogue.

2. Materials and Methods

2.1 Chemicals, Reagents, and Antibodies

Sigma-Aldrich (Sigma-Aldrich, Inc., St. Louis, MO, USA) provided phosphate buffered saline (PBS), L-glutamine, DMEM, Tween 20, and DNase I. Invitrogen ((Invitrogen, Grand Island, NY, USA) provided penicillin-streptomycin mixture, while Biosolutions International provided the fetal bovine serum (FBS, Biosolutions International, Melbourne, Australia). Roche (Roche, Mannheim, Baden-Württemberg, Germany) provided the protease inhibitor cocktail. Therrmo Fisher Scientific Life Sciences (Waltham, MA, USA) provided TRizol® reagent, Diethylpyrocarbonate (DEPC), RNA Later, the Revert aid RNA reverse transcription kit, and the maxima SYBR green qPCR kit. Santa Cruz Biotechnology (Santa Cruz, CA, USA) provided the primary antibodies against *AKT*, *PI3K*, *ERK1/2*, *MEK1/2*, *p-AKT*, *p-PI3K*, *extracellular signal-regulated kinase1/2* (*p-ERK1/2*), *mitogen-activated protein kinase kinases 1/2* (*p-MEK1/2*), and *β-actin*. Horseradish peroxidase (HRP)-conjugated secondary antibodies were obtained from Life Technologies Japan (Minato-Ku, Tokyo, Japan). CA4-P was purchased from Bolise Co. (Qingpu District, Shanghai, China).

2.2 Chemistry

The examined compound, the CA-4 analogue, was prepared using the Schotten Baumann reaction and Sawdey rearrangement as per the instructions provided in our previous work. As previously reported, the molecule was characterized using 1H-NMR and 13C-NMR [24].

2.3 Cell Culture and Reagents

MCF7 (ER+/PR+/HER2-), MDA-MB231 (ER-/PR-/HER2-), and MDA-MB453 (ER-/PR-/HER2+) breast cancer cell lines were obtained from ATCC (CCL-2, Manassas, VA, USA). Cells were grown in fresh DMEM sup-

plemented with L-glutamine (10 g/L), 10% FBS, and a penicillin-streptomycin solution (10 g/L). The authenticity of cell lines used in the study was verified through short tandem repeat profiling. Cells were routinely tested for mycoplasma contamination using the 4',6-diamidino-2-phenylindole (DAPI) staining method. All cell lines tested negative for mycoplasma.

The cells were cultivated at 37 °C in a 5% CO_2 humid incubator. Just before use, CA-4 and its analogue were dissolved in the culture medium to the required concentrations.

2.4 Cell Proliferation Assay

Cell survival was evaluated using 3-(4,5-dimethylthiazol-2-yl)-2,5 diphenyl-2H-tetrazolium bromide (MTT) assay. The cells were cultivated (1×10^4 cells/well) in a 96-well plate. After 24 hours of incubation in a freshly prepared DMEM media, the cells underwent treatment with sequential concentrations (0–1000 µg/mL) of CA-4 or the CA-4 analogue in fresh DMEM for 48 hours. Subsequently, the cells were subjected to 10 µL MTT solution (5 g/mL) and cultivated in dark conditions for 4 hours. Subsequently, 100 µL of Dimethyl sulfoxide (DMSO) was added to dissolve the formazan crystals that had been produced. The visual density at 570 nm was assessed using an Enzyme-linked immunosorbent assay (ELISA) plate reader (Bio-Rad, Hercules, CA, USA). The cell viability at various concentrations was estimated by comparing it to cells treated solely with the medium [25,26]. The half maximum inhibitory concentration (IC_{50}) was determined using the dosage response curve equation with graphPad Prism 7 software (GraphPad Software Inc., San Diego, CA , USA).

2.5 Apoptosis Determination Using Annexin V-Fluorescein isothiocyanate/Propidium iodide (FITC/PI) Staining

Cellular apoptosis was detected using flow cytometry following the manufacturer's instructions (Immunotech, Marseille, France) and using the Apoptosis detection kit. In triplicate, cells (5×10^5 cells) were harvested in Dulbecco's Modified Eagle Medium (DMEM) medium and cultured at 37 °C in a 5% CO_2 incubator for 24 hours to allow attachment. The medium was then replaced with DMEM containing the tested compound (IC_{50}), and the cells were cultivated for 48 hours before being harvested. Cells were rinsed with cold PBS and remixed with the binding buffer. Subsequently, labeled annexin V and PI were added to the cells at 4 °C for 30 minutes in the dark for cell staining [27]. The FACS Calibur flow cytometer (Becton Dickinson, Franklin Lakes, NJ, USA) was used to analyze at least 10^4 cells. As previously reported, dot plots were generated, and the proportion of total apoptosis was assessed [28].

2.6 Molecular Docking

The molecular docking and visualization processes were conducted on the binding site of Epidermal growth factor receptor (EGFR) using Molecular Operating Environment (MOE) 2019.0102. RCSB Protein Data Bank was used to retrieve the co-crystal structure. The CA-4 analogue was prepared using the standard protocol in MOE, and the energy of the docked compound was reduced with a gradient RMS of 0.0001 kcal/mol. The structure of the protein was generated using the QuickPrep protocol in MOE. The co-crystallized ligand was redocked using the same set of variables mentioned earlier to validate the docking study at the active site [29–31]. The best-docked pose exhibited a root mean square deviation (RMSD) value of 0.9472 Å, confirming the accuracy of the docking study with MOE software 2019.01 (Chemical Computing Group, Montreal, QC, Canada). The CA-4 analogue was docked into the EGFR binding site using the alpha triangle placement method with the Amber10: EHT forcefield. The refinement was done with the Forcefield, and the docking results were scored using the Affinity dG scoring system.

2.7 RNA Isolation and Quantification

A total of 5×10^5 cells have been cultivated in triplicate on a 6-well plate. The cells have been then cultured in DMEM medium under controlled conditions of 5% CO_2 and 37 °C temperature for 24 hours. Following that, the medium was replaced with DMEM containing the CA-4 analogue at its IC_{50} concentration, and the cells have been further maintained for another 24 or 48 hours before being collected. For total RNA isolation from both the treated and untreated cells, TRizol® (Invitrogen, USA) was used according to the guidelines provided by the manufacturer [32]. Nano-Drop 1000 (Thermo Scientific, Waltham, MA, USA) was employed to determine the quality and amount of the obtained RNA [33].

2.8 Analysis of Genes Expression by Real Time-PCR

As per the guidelines provided by the manufacturer, a high-capacity reverse transcriptase kit was utilized to reverse transcribe the mRNA pool using random hexamer primers. The reverse transcription reaction was carried out with a cycle of ten minutes at 25 °C, followed by incubation for 120 minutes at 37 °C, and finally incubation for 5 minutes at 85 °C to ensure completion. For quantitative real time-polymerase chain reaction (qRT-PCR), the resultant cDNA was used with the Maxima SYBR Green qPCR master mix (Thermo Scientific, USA). The protocol included a 10-minute initial denaturation phase at 95 °C, followed by 30 amplification cycles consisting of 15 seconds at 95 °C, 30 seconds at 60 °C, and 30 seconds at 72 °C. A final 10-minute extension step at 72 °C was included. Following the manufacturer's protocol, a Step One Real-Time PCR System (Thermo Fisher, USA) was used to perform the amplification [34,35]. All analyses were conducted in

Table 1. PCR primers of assessed genes.

Primer		Sequence
GAPDH	Forward	5′-CGGGGCTCTCCAGAACATCAT-3′
	Reverse	5′-GTCCACCACTGACACGTTGG-3′
Bcl-2-associated X protein (*Bax*)	Forward	5′-CTGCAGAGGATGATTGCCGC-3′
	Reverse	5′-GGGCGTCCCAAAGTAGGAGA-3′
B-cell lymphoma 2 (*Bcl2*)	Forward	5′-CTGGTGGACAACATCGCCCT-3′
	Reverse	5′-GCCGTACAGTTCCACAAAGGC-3′
P53	Forward	5′-GGTGACACGCTTCCCTGGAT-3′
	Reverse	5′-CATCCATTGCTTGGGACGGC-3′

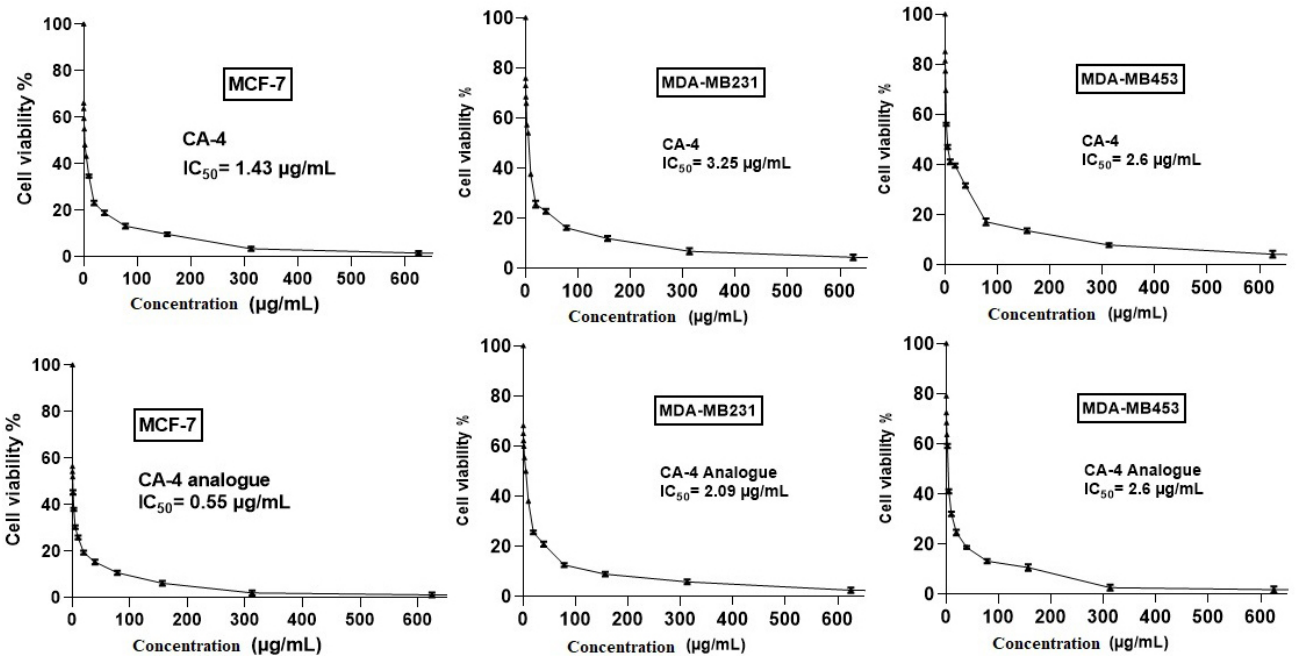

Fig. 2. Cell viability assay. Impact of CA-4 and CA-4 analogue on the viability of MCF-7, MDA-MB231, and MDA-MB453 cells following treating the cells for 48 hours. The cell survival rates are calculated as a percent of untreated cells, and results are calculated from three independent experiments.

triplicate, and the housekeeping gene *Glyceraldehyde-3-phosphate dehydrogenase* (*GAPDH*) was used as a reference in all experiments. The obtained qRT-PCR data were evaluated using the $\Delta\Delta$Ct method. The fold changes of treated cells were determined by comparing them to the untreated cells: fold change = $2^{-\Delta\Delta Ct}$ [36]. Table 1 contains the primer sequences.

2.9 Western Blot Assay of Protein Expression

Protein expression was assessed using sodium dodecyl sulfate–polyacrylamide gel electrophoresis (SDS-PAGE) and immunoblotting techniques. Cells were cultured in triplicate at an average number of 2×10^5 cells/well on a six-well plate. After 24 hours of cultivation in a freshly prepared DMEM media, the cells were subjected to a medium containing CA-4 or CA-4 analogue (at their respective IC_{50} concentrations) for 24 or 48 hours. All cells, including both attached and floating cells, were collected, washed, and centrifuged to obtain a cell pellet. Protein extraction was performed using the Ready Prep TM protein extraction kit as instructed by the manufacturer (Bio-Rad Inc, Catalog #163-2086). Bradford assay kit (SK3041, Bio basic Inc, Markham, Ontario, Canada) was used to assess the protein level of each sample. SDS-PAGE (15% acrylamide gel) was used to resolve 20 µg of total protein from each sample before transferring it to polyvinylidene fluoride (PVDF) membranes (Millipore). After membrane blocking, primary antibodies against MEK (sc-81504), p-MEK (sc-81503), ERK1/2 (sc-135900), p-ERK (sc-136521), AKT (SC-5298), P-AKT (SC-514032), PI3K (SC-423), p-PI3K (SC-12929), and β-actin (sc-47778) were added. After 4 °C overnight incubation, HRP-labelled secondary antibodies were used. As instructed by the manufacturer, immunoreactive proteins were estimated using a chemiluminescent substrate. A camera equipped with a CCD sensor was utilized to track chemiluminescent signals (LAS4000, Fuji-

film Co., Tokyo, Japan). Three separate immunoblots were performed for each protein. β-actin served as a housekeeping protein. Densitometric analysis was carried out using the ImageJ program (NIH, Bethesda, Maryland, USA) [37].

2.10 Statistical Analysis

Data were demonstrated as mean ± SEM. A one-way ANOVA test was carried out to assess the statistical relevance of the differences. Post hoc Tukey's was performed for inter-group comparison using GraphPad Prism 7 program (GraphPad Software Inc., San Diego, CA, USA). When the p-value was less than 0.05, differences were regarded as significant.

3. Results

3.1 In vitro Antiproliferative Assay

The potential anticancer activity of CA-4 and its analogue were investigated in three distinct breast cancer cell lines: MCF-7, MDA MB-231, and MDA MB-453. MTT assays were performed to assess cell growth suppression after a 48-hour incubation period. Both CA-4 and its analogue exhibited dose-dependent attenuation of cell proliferation in all three cell lines. Notably, the results highlighted the anticancer potential of CA-4 against MCF-7, MDA MB-231, and MDA MB-453 cells, with respective IC_{50} values of 1.43 µg/mL, 3.25 µg/mL, and 4.93 µg/mL. However, the newly synthesized CA-4 analogue exhibited an even greater anti-proliferative impact, with IC_{50} values of 0.55 µg/mL, 2.09 µg/mL, and 2.6 µg/mL for each respective cell line. Particularly, MCF-7 exhibited the highest susceptibility to the cytotoxicity of both compounds, and the CA-4 analogue displayed a significantly lower IC_{50} compared to its parent compound ($p < 0.05$). These exciting findings suggest varying sensitivities of the three cancer cell lines towards the cytotoxicity of the CA-4 analogue, with MCF-7 being the most responsive cell line (Fig. 2 and Table 2).

Table 2. IC_{50} (µg/mL) values for CA-4 analogue against MCF-7, MDA-MB231, and MDA-MB453 cell lines compared to CA-4.

Cell line	CA-4 analogue	CA-4
MCF-7	0.55 *	1.44
MDA-MB231	2.09 *f*	3.25
MDA-MB453	2.6 #	4.93

*: p-value < 0.05 comparing to CA-4 treated MCF-7 cells, *f*: p-value < 0.05 comparing to CA-4 treated MDA-MB231 cells and #: p-value < 0.05 comparing to CA-4 treated MDA-MB453 cells.

3.2 The Cytotoxic CA-4 Analogue-Induced Cell Apoptosis

The results presented in Fig. 3 demonstrate the remarkable ability of CA-4 and its analogous compounds to induce apoptosis in MCF-7, MDA-MB231, and MDA-MB453 cells. After 48-hour treatment with CA-4, the percentage of cellular apoptosis was 27.89 ± 2.1%, 21.07 ± 1.3%, and 18.51 ± 1.5% in MCF-7, MDAMB231, and MDA-MB453 cells, respectively, with a significant elevation ($p < 0.0001$) observed in each cell type. Similarly, following a 48-hour treatment with CA-4 analogue, the percentage of cellular apoptosis significantly increased ($p < 0.0001$) to 39.89 ± 1.5%, 32.82 ± 0.6% and 23.77 ± 1.1% in MCF-7, MDA-MB231, and MDA-MB453 cells, respectively, in comparison with untreated cells. These findings emphasize the potent apoptotic activity of CA-4 and its analogue compound in these cells, shedding light on their potential therapeutic applications.

3.3 Molecular Docking

To further rationalize the potent inhibitory activity of CA-4 analogue on EGFR kinase, molecular docking was performed on the crystal structure of the EGFR kinase domain (PDB code: 1M17) in complex with erlotinib [38]. CA-4 analogue displayed several essential interactions within the active site of EGFR and showed better interaction energy than the native ligand erlotinib; the carbonyl oxygen formed a hydrogen bond with the key amino acid Met769, the p-methoxy group showed two hydrogen bonds with Met742 and Glu738, and the m¬-choro group formed a hydrogen bond with Asn818 of the catalytic loop (Table 3, Fig. 4). Further, the synthetic derivative showed a hydrophobic interaction with Asp831 of the DFG motif, while Leu820, Val702, and Leu694 showed several π..H contacts with the 1,2,4-triazole and the phenyl rings.

3.4 CA-4 Analogue Inhibited the PI3K/AKT Pathway and Downstream Protein Expression

Treatment of MCF-7 cells with CA-4 analogue for 24 and 48 hours led to a significant time-dependent decrease ($p < 0.0001$) in the protein levels of p-PI3K/t-PI3K (0.26 and 0.12, respectively) and p-AKT/t-AKT (0.28 and 0.11, respectively) in comparison with control cells. Correspondingly, treatment of MCF-7 with CA-4 for 24 and 48 hours resulted in a substantial decrease ($p < 0.0001$) in p-PI3K/t-PI3K and p-AKT/t-AKT levels, showing reductions of approximately 0.56 and 0.29 for p-PI3K and 0.62 and 0.17 for p-AKT, respectively, relative to the untreated control cells. Interestingly, there was a significant difference in the protein levels of p-PI3K and p-AKT between cells treated with the CA-4 analogue and CA-4 for 24 hours and 48 hours ($p < 0.0001$) (Fig. 5).

Furthermore, following CA-4 analogue treatment, MDA-MB 231 cells exhibited dramatically lowered p-PI3k and p-AKT levels relative to t-PI3k and t-AKT proteins in a time-dependent manner in comparison with untreated cells. Treatment of MDA-MB231 cells with the CA-4 analogue for 24 or 48 hours resulted in the attenuation of p-PI3k (0.6 and 0.2) ($p < 0.0001$) and p-AKT (0.6 and 0.26)

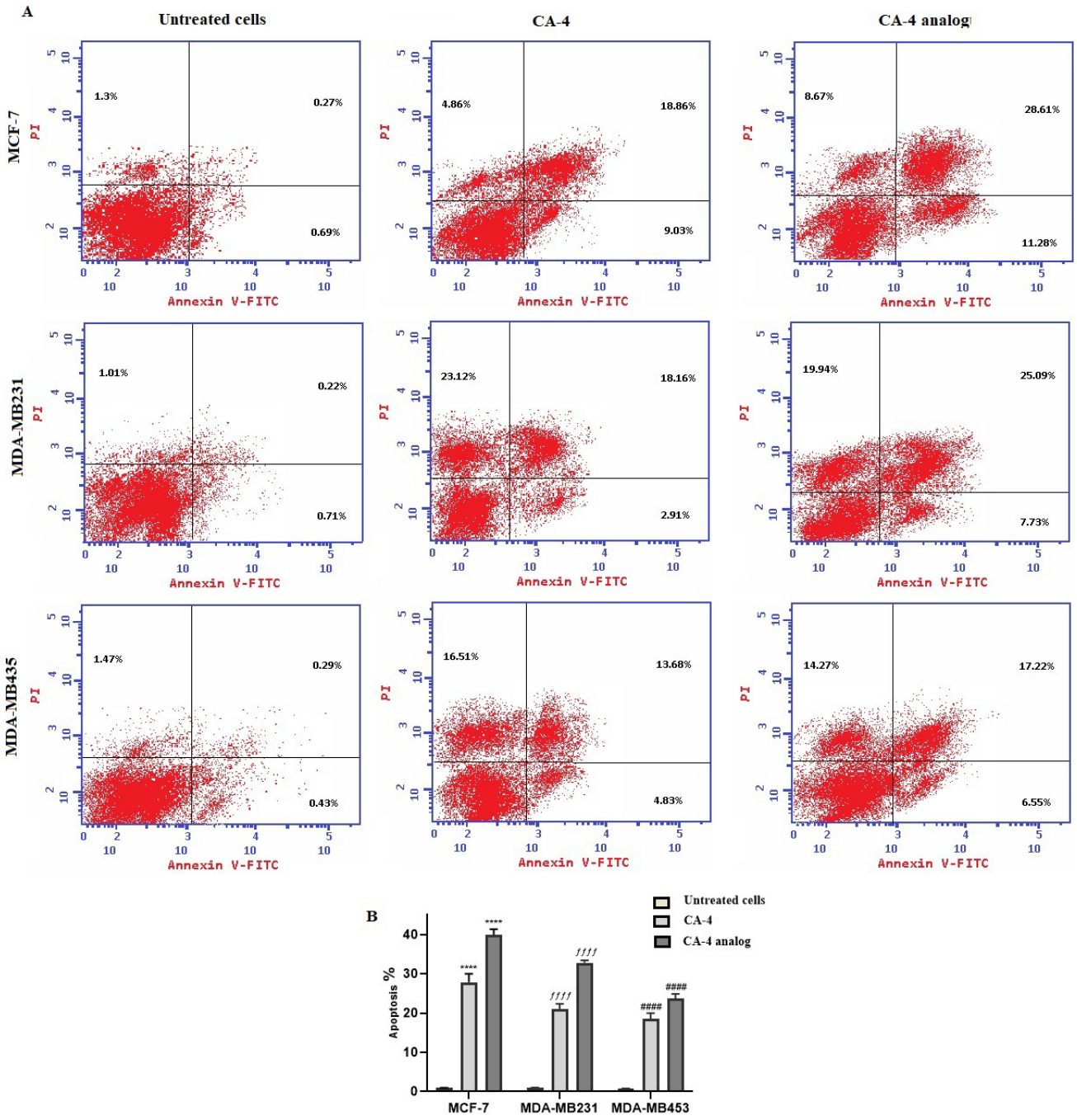

Fig. 3. Impact of CA-4 and its analogue on apoptosis in MCF-7, MDA-MB231, and MDA-MB453 cancer cell lines was assessed using Annexin V assay. (A) The dot plots depict the MCF-7, MDA-MB231, and MDA-MB453 cancer cell lines. (B) The proportion of apoptotic cells in breast cancer cell lines was determined after 48 hours of treatment with CA-4 or its derivative (IC_{50}). The presented data are expressed as mean ± SEM. Statistical significance of the difference was evaluated using a one-way ANOVA test, where: ****: $p < 0.0001$ relative to MCF-7 untreated cells; $ffff$: $p < 0.0001$ relative to MDA-MB231 untreated cells; ####: $p < 0.0001$ relative to MDA-MB453 untreated cells.

($p < 0.0001$), as illustrated in Fig. 5. Moreover, CA-4 significantly decreased p-PI3k (0.6 and 0.3) ($p < 0.001$) and p-AKT (0.68 and 0.4) ($p < 0.0001$) in 24 or 48 hours treated cells, respectively, compared to control cells. There was a considerable difference between CA-4- and CA-4 analogue-treated cells in p-AKT levels after 24 hours of incubation ($p < 0.001$). Additionally, there was significant variance between cells treated with CA-4 or its analogue for 48 hours ($p < 0.0001$) in terms of p-AKT and p-PI3k. There was no statistical difference in p-PI3K levels at 24 hours between CA4 and CA-4 analogue treated cells (Fig. 5).

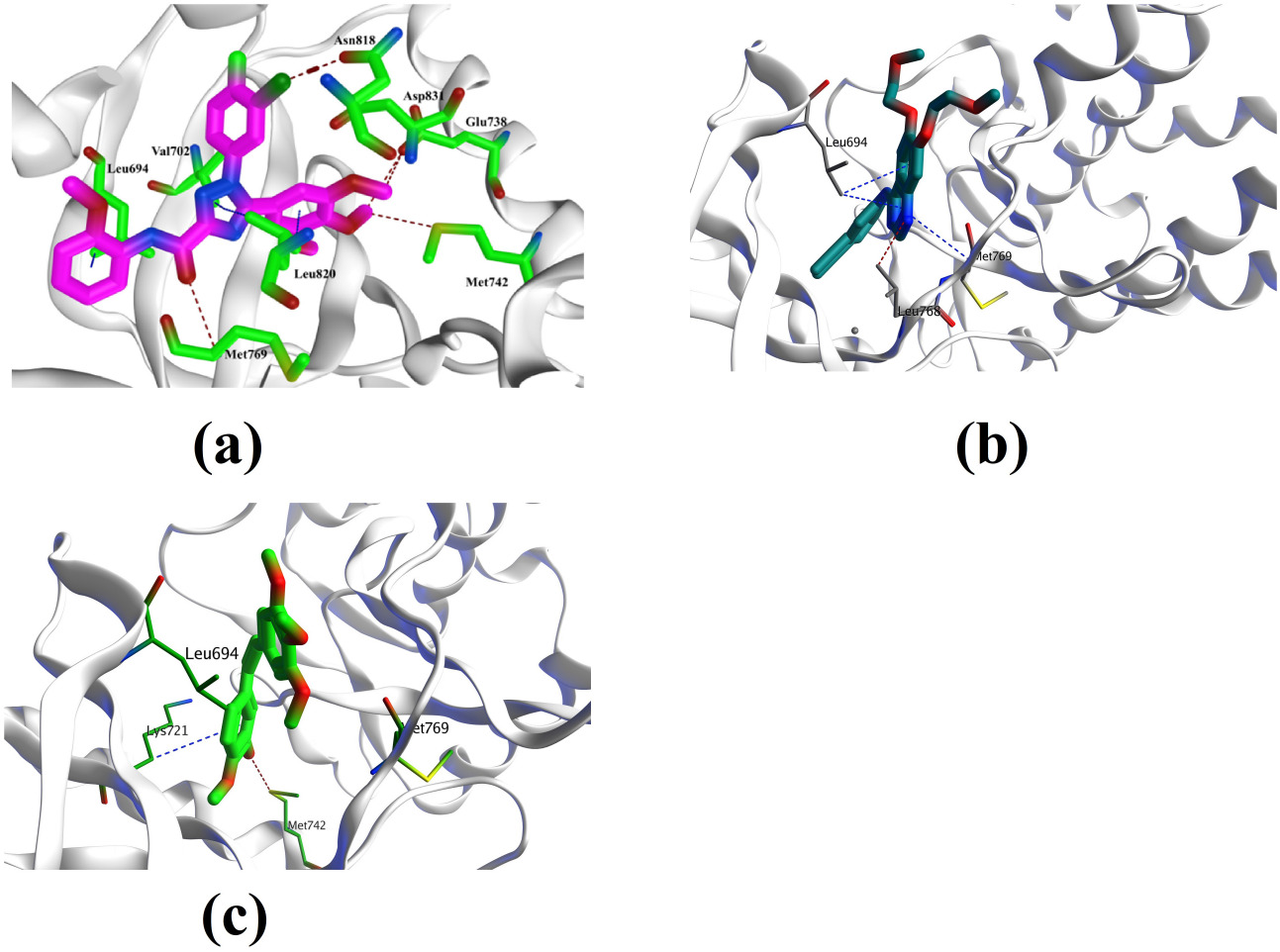

Fig. 4. 3D representation and interactions of (a) CA-4 analogue, (b) erlotinib, and (c) CA-4 within the EGFR active site.

Table 3. Energy scores (kcal/mol) and binding features for CA-4 and CA-4 analogue compared to erlotinib, within EGFR binding site.

Compound	Energy score (S) (kcal/mol)	Ligand-receptor interactions		
		Residue	Type	Length (Å)
Erlotinib	–8.21	Met769	Hydrogen bond	4.03
		Met742	Hydrogen bond	4.25
		Leu768	Hydrogen bond	4.03
		Gln767	Hydrogen bond	3.34
		Leu694	π..H	3.92
		Val702	π..H	7.78
CA-4 analogue	–8.89	Met769	Hydrogen bond	3.57
		Met742	Hydrogen bond	3.64
		Asn818	Hydrogen bond	3.15
		Leu694	π..H	3.75
		Val702	π..H	4.47
		Leu820	π..H	3.64
CA4	–6.87	Glu738	Hydrogen bond	3.46
		Leu694	π..H	4.70
		Leu694	π..H	4.57
		Val702	π..H	4.58
		Gly772	π..H	4.83

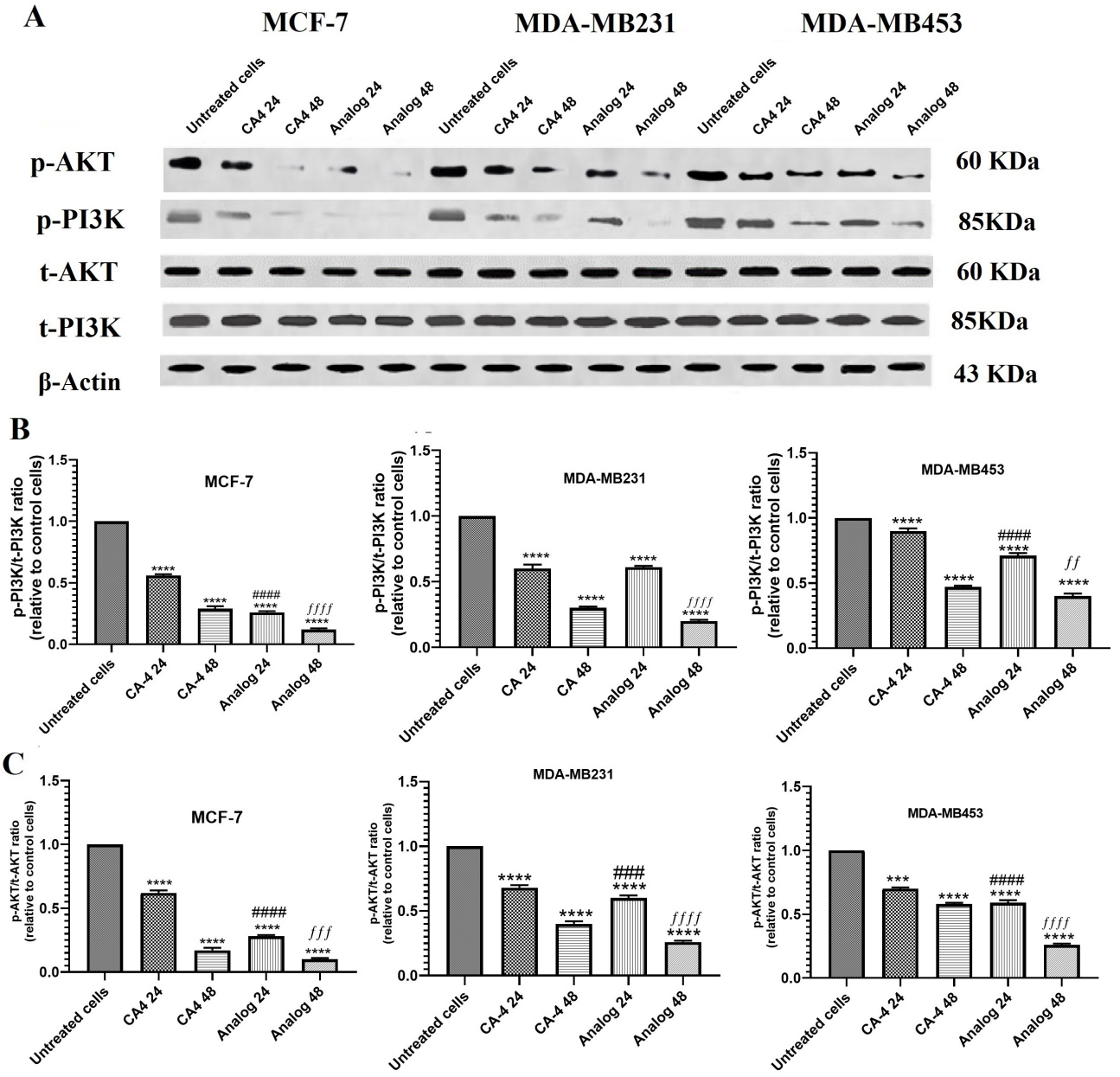

Fig. 5. Effect of CA-4 and CA-4 analogue on PI3k/AKT pathway in MCF-7, MDA-MB231, and MDA-MB453 cells. (A) Representative immunoblots of p-PI3k, tPI3k, p-AKT, and t-AKT in MCF-7, MDA-MB231, and MDA-MB453 cells treated with the IC_{50} concentration of CA-4 or CA-4 analogue for 24 or 48 hours. β-actin was used as an internal loading control. β-actin was included as an internal reference. (B,C) The protein expression in treated cells was displayed in comparison with untreated cells, following normalization to the corresponding β-actin expression. Results are shown as mean $\pm$ SEM. The significant variance between groups was calculated by one-way ANOVA and post hoc Tukey's test, where: ***: $p < 0.001$, ****: $p < 0.0001$, compared to untreated cells; ####: $p < 0.0001$, ###: $p < 0.001$, compared to CA-4 24 treated cells; and $ffff$: $p < 0.0001$, fff: $p < 0.001$, ff: $p < 0.05$, compared to CA-4 48 treated cells. Results are calculated from three independent experiments.

Furthermore, MDA-MB453 cells displayed significantly lower levels of p-PI3K (0.71 and 0.4) and p-AKT (0.59 and 0.26) after 24 or 48 hours of CA-4 analogue treatment ($p < 0.0001$). The suppression of PI3K and AKT phosphorylation was shown to be time-dependent. MDA-MB453 cells exhibited significantly downregulated expression of p-PI3K (0.9 and 0.47) and p-AKT (0.7 and 0.58) following CA-4 treatment, respectively, as illustrated in Fig. 5. The difference between cells treated with CA-4 or its analogue for 24 hours was significant ($p < 0.0001$) for both p-AKT and p-PI3K. Moreover, the difference was statistically significant between cells treated with CA-4 or its analogue for 48 hours for p-AKT ($p < 0.0001$) and for p-PI3K ($p < 0.01$).

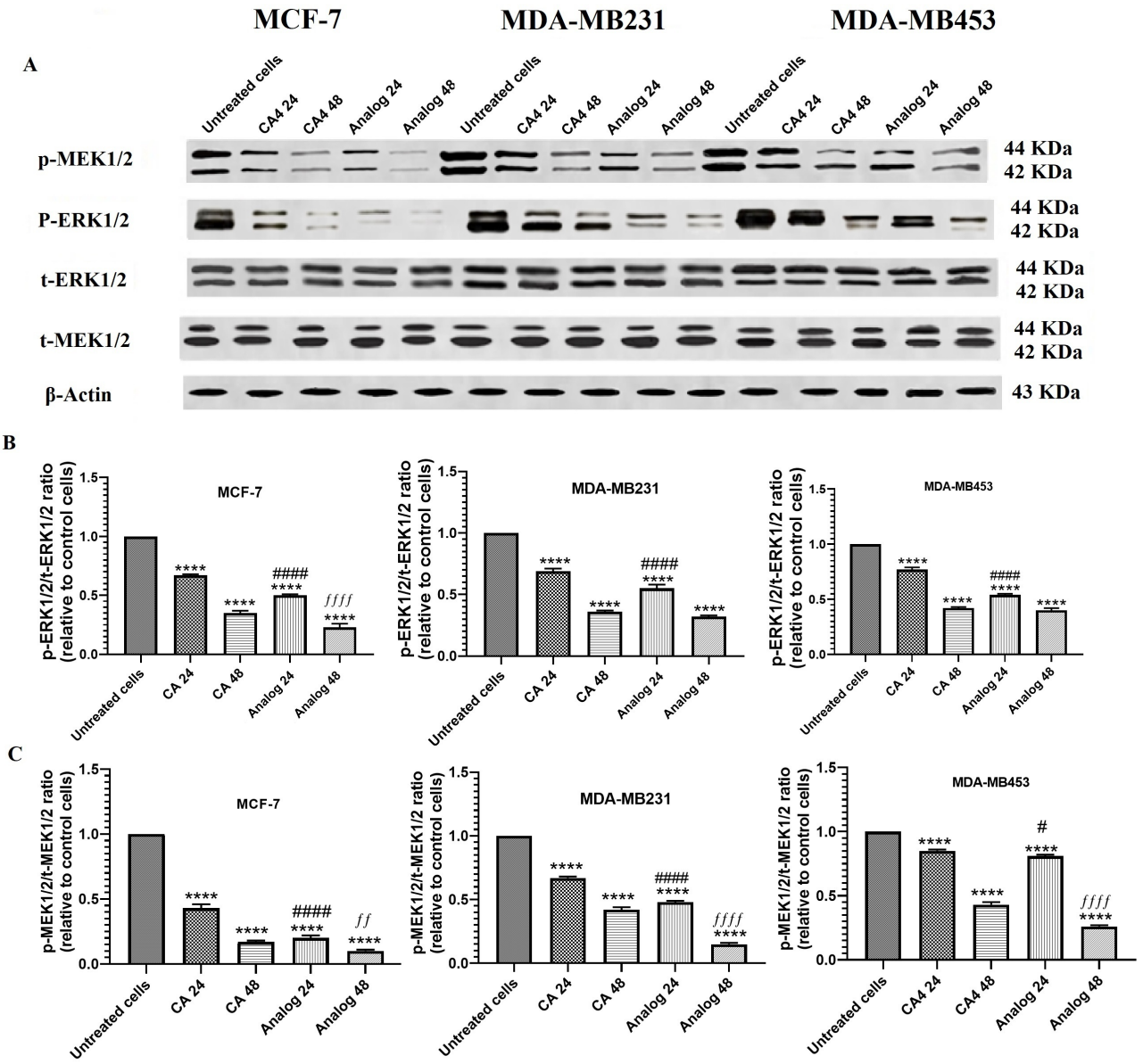

Fig. 6. Impact of CA-4 and CA-4 analogue on MAPK/ERK pathway MCF-7, MDA-MB231, and MDA-MB453 cells. (A) Representative blots of p-MEK1/2, tMEK1/2, p-ERK1/2, and t-ERK1/2 in MCF-7, MDA-MB231, and MDA-MB453 cells treated with the IC_{50} concentration of CA-4 or CA-4 analogue for 24 or 48 hours. β-actin has been employed as a loading control. (B,C) Protein expression in treated cells was represented relative to untreated cells following normalization to the corresponding β-actin expression. Results are shown as mean $\pm$ SEM. Using one-way ANOVA and the post hoc Tukey's test, a significant difference between the groups was obtained, where: ****: $p < 0.0001$, relative to untreated cells; ####: $p < 0.0001$, #: $p < 0.05$, relative to CA-4 24 treated cells; and $ffff$: $p < 0.0001$, ff: $p < 0.01$ relative to CA-4 48 treated cells. Results are calculated from three independent experiments.

3.5 CA-4 Analogue Inhibited the MAPK/ERK Pathway and the Downstream Protein Expression

We then evaluated the *in vitro* effect of the tested substances on the MAPK/ERK pathway by treating various breast cancer cells with the tested compounds at IC_{50} concentrations for 24 and 48 hours. Fig. 6 shows representative immunoblots of protein expression (t-MEK1/2, t-ERK1/2, p-MEK1/2, and p-ERK1/2) in MCF-7, MDA-MB-231, and MDA-MB-453 cells.

The findings revealed that CA-4 analogue significantly decreased p-MEK1/2/t-MEK1/2 ratio and p-ERK1/2/t-ERK1/2 ratio ($p < 0.0001$) after 24- and 48-hour treatment to 0.2 and 0.1 for p-MEK1/2/t-MEK1/2 and 0.51 and 0.23 for p-ERK1/2/t-ERK1/2, respectively, comparing to untreated cells. Meanwhile, CA-4 significantly ($p < 0.0001$) decreased p-MEK1/2 (0.43 and 0.17) and p-ERK1/2 (0.76 and 0.35), respectively, compared to control cells (Fig. 6). The decrease was shown to be statistically

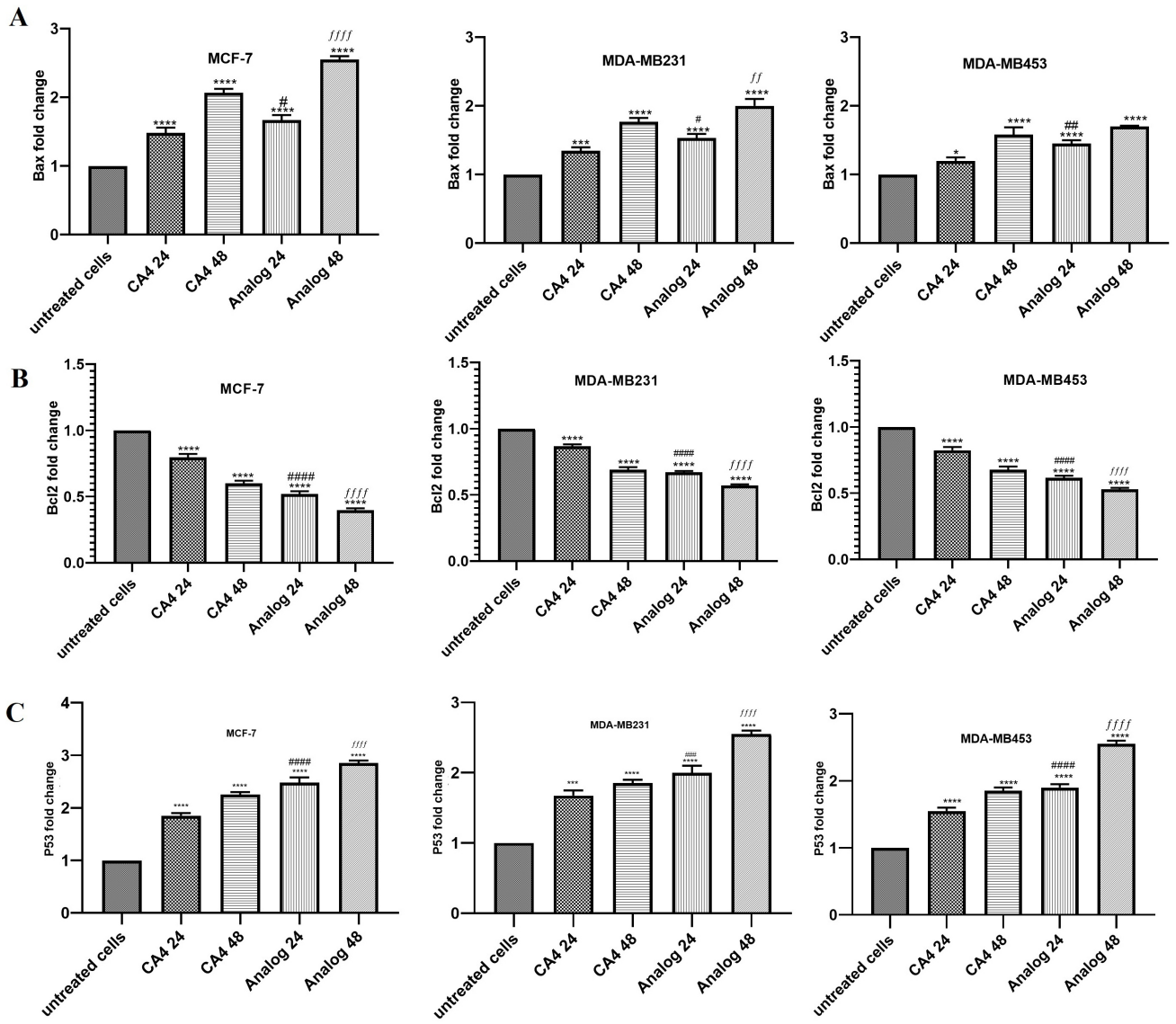

Fig. 7. Impact of CA-4 and CA-4 analogue on (A): *Bax*, (B): *Bcl2*, and (C): *P53* genes' expression in MCF-7, MDA-MB-231 MDA-MB453 cells. Relative gene expression in all cells treated with the IC_{50} concentration of CA-4 or CA-4 analogue for 24 or 48 hours relative to untreated cells. Expression was normalized to GAPDH housekeeping gene expression. Bars represent mean $\pm$ SEM. Significant difference was analyzed by two-way ANOVA and post hoc Tukey's test: *: $p < 0.05$, ***: $p < 0.001$, ****: $p < 0.0001$, relative to untreated cells; ####: $p < 0.0001$, relative to CA-4 24 treated cells; ###: $p < 0.001$, relative to CA-4 24 treated cells; ##: $p < 0.01$ relative to CA-4 24 treated cells; #: $p < 0.05$ relative to CA-4 24 treated cells; $ffff$: $p < 0.0001$ relative to CA-4 48 treated cells; and ff: $p < 0.01$ relative to CA-4 48 treated cells. Results were calculated meticulously from three independent experiments.

significant between CA-4- and CA-4 analogue-treated cells for p-ERK1/2 ($p < 0.0001$) and p-MEK1/2 ($p < 0.01$) at both 48 and 24 hours of treatment ($p < 0.0001$) for both p-MEK1/2 and p-ERK1/2.

In MDA-MB-231 cells, CA-4 analogue significantly ($p < 0.0001$) suppressed the phosphorylation of MEK1/2 (0.48 and 0.15) and ERK1/2 (0.55 and 0.32) following treatment for 24 and 48 hours, respectively, in comparison with control cells. CA-4 also significantly ($p < 0.0001$) suppressed the phosphorylation of MEK1/2 (0.67 and 0.42) for 24 and 48 hours, and ERK1/2 (0.69 and 0.36) for 24 and 48 hours, in a time-based approach (Fig. 6). There was a considerable difference between CA-4- and CA-4 analogue-treated cells for 24-hours regarding both proteins ($p < 0.0001$) and at 48-hours treatment, there was a significant difference between CA-4 and its analogue for MEK1/2 only ($p < 0.0001$).

The MDA-MB453 cells exhibited markedly low levels of p-MEK1/2 (0.81 and 0.26) and p-ERK1/2 (0.54 and 0.4) after CA-4 analogue treatment for 24 and 48 hours, respectively. Meanwhile, CA-4 significantly attenuated p-MEK1/2 (0.85 and 0.43) and p-ERK1/2 (0.77 and 0.42) af-

ter 24 and 48 hours of treatment, respectively. The suppression of ERK1/2 and MEK1/2 phosphorylation was shown to be time-dependent (Fig. 6). The suppression was statistically significant between CA-4- and CA-4 analogue-treated cells at 24 hours (p-ERK: $p < 0.001$ and p-MEK: $p < 0.05$), as well as in 48 hours treated cells specifically for p-MEK ($p < 0.0001$).

3.6 CA-4 Analogue Induces Apoptosis by Increasing P53 and Bax and Inhibiting Bcl2 Gene Expression

The MCF-7, MDA MB-231, and MDA MB453 cell lines were administered the IC_{50} dose of a CA-4 analogue for 24 or 48 hours. Treatment of MCF-7 cells with the CA-4 analogue for 24 or 48 hours resulted in a significant time-dependent upregulation of *P53* gene expression, showing a 2.45- and 2.85-fold increase, respectively, in comparison with untreated cells ($p < 0.001$). Correspondingly, treating the MDA MB-231 cells with the CA-4 analogue for 24 or 48 hours also led to a time-dependent upregulation of *P53* gene transcription, with a 2- and 2.25-fold increase, respectively. Similar upregulation was observed in the MDS MB-453 cells, in which CA-4 analogue exerted a 1.9- and 2.55-fold increase in *P53* gene transcription after 24 or 48 hours of treatment compared to untreated cells.

The *Bax* mRNA expression was upregulated, while the *Bcl2* levels were reduced in the tested breast cancer cells after CA-4 analogue treatment for 24 or 48 hours. Overall, our experimental data demonstrated that the CA-4 analogue may promote apoptosis in breast cancer cells in a time-dependent approach. Furthermore, gene expression analyses conducted on MCF-7, MDA-MB231, and MDA-MB453 cells revealed that both CA-4 and the CA-4 analogue dramatically elevated the ratio of Bax to *Bcl2*. The impact was particularly pronounced in cells treated with the CA-4 analogue compared to those treated with CA-4 alone (Fig. 7).

4. Discussion

Breast cancer is the most predominant form of female malignant tumors. Extensive research has been conducted to explore innovative treatment options [39]. Despite the availability of current treatments for various breast cancer subtypes, their effectiveness is limited due to resistance and unsatisfactory outcomes. Consequently, overall patient survival rates have not shown improvement [4,40]. This necessitates identifying new therapeutic candidates overcoming treatment failure for optimizing effective therapy and improving survival rate. Despite the *in vitro* cytotoxic effect of the parent CA-4 on multiple cancer cell lines, *in vivo* studies have revealed a dramatic decline in its antiproliferative activity due to spontaneous isomerization to the more stable trans-isomer.

Several CA-4 derivatives have been designed and assessed for their anticancer activity. Among them, one derivative has shown prominent cytotoxic activity against MCF-7 breast cancer cells [24]. These findings have motivated us to investigate further the potential cytotoxic effects of this promising compound in different types of breast cancer cell lines and to explore the plausible molecular mechanism responsible for its remarkable activity.

The current results demonstrate that the CA-4 analogue exhibits a remarkable dose-dependent inhibitory impact on the survival of breast cancer cells, with IC_{50} values lower than those of the parent CA-4. The enhanced cytotoxic activity of the newly synthesized CA-4 analogue is evidently due to the substitution of the hydroxyl group in CA-4 with chlorine in the meta-position of ring B. Additionally, the replacement of the para-methoxy group in CA-4 with a fluorine substitution in the analogue significantly improves its cytotoxic activity. Furthermore, the introduction of an extension to the structure (ring C) enhances the potency, particularly with ortho-methoxy substitution [24]. Notably, the CA-4 derivative exhibited more potent antiproliferative activity against MCF-7 with the lowest IC_{50} values, compared to MDA-MB231 and MDA-MB453 cells. This observation may be attributed to the substantial overexpression of EGFR in MDA-MB231 cells, the TNBC cell line, which promotes cancer cell survival and inhibits apoptosis [41]. Whilst, MDA-MB453 cells are characterized by significantly upregulated, constitutively dimerized, and activated HER-2 receptors, providing alternative pathways for sustained neoplastic cell proliferation, thus making these breast cancer subtypes more aggressive and invasive [42].

Apoptosis induction has been proposed as an effective strategy for cancer therapy [43–45]. The extrinsic death receptor pathway, as well as the mitochondrial intrinsic pathway, were both engaged in the triggering of cellular apoptosis [46]. Numerous defense mechanisms have been established by cancer cells to combat apoptotic cell death. One such mechanism is the overexpression of antiapoptotic *Bcl2*, which promotes enhanced tumor cell proliferation and inhibits apoptosis [44]. Conversely, elevated expression of *Bax* promotes cell death and hence eradicates tumor cells [47,48].

During the last ten years, there has been increasing interest in targeting *P53*, a crucial protein involved in suppressing tumor growth, as a potential strategy for cancer treatment. This interest stems from the ability of *P53* to control different cellular mechanisms such as DNA repair, cellular apoptosis, and cell cycle arrest [49]. Activation of the *P53* protein can increase the sensitivity of cancer cells to DNA damage, preventing their replication and promoting apoptosis [50]. In our study, we observed that the novel CA-4 derivative induced upregulation of p53 expression in MCF-7, MDA MB231, and MDA MB453 cells. Additionally, the derivative enhanced apoptosis by elevating the expression of *Bax*, while decreasing that of *Bcl2*. This led to an increased *Bax/Bcl2* ratio, which can trigger the collapse of the mitochondrial membrane, the release of cytochrome c, and ultimately cellular apoptosis [25,48]. Our investi-

gation revealed that treatment with the CA-4 analogue resulted in a time-dependent increase in the ratio of *Bax/Bcl2* after 24 and 48 hours, suggesting that the CA-4 analogue induces apoptosis through the mitochondrial pathway. This observation was consistent with the evident elevation in the apoptotic cell population, as demonstrated by annexin V/PI dual staining. The percentage of apoptotic cells (Annexin-V positive) was highest in MCF-7 cells relative to MDA-MB-231 and MDA-MB453 cells.

To better understand the mechanism of action of the new CA-4 analogue, *in vitro* molecular docking was conducted on EGFR binding sites. The upregulation of the EGFR signaling pathway has been associated with reduced apoptosis, which directly contributes to cancer development, tumorigenesis, increased cell proliferation, and angiogenesis [51]. The EGFR gene is expressed in approximately 14–91% of breast carcinomas, and its dysregulation is associated with more invasive breast tumor subtypes and poorer prognoses [52]. Moreover, EGFR can activate signaling cascades such as the MAPK/ERK and PI3K/AKT pathways to transmit its signal, making it a potential target for controlling cancer cell proliferation. Through *in vitro* molecular docking, the CA-4 analogue demonstrated potent inhibitory activity against EGFR kinase. The CA-4 analogue exhibited several critical interactions within the active site of EGFR. This observed potent inhibitory activity of CA-4 analogue explains its cytotoxic activity towards tested breast cancer cells [42].

The PI3K/AKT signaling pathway is frequently associated with breast carcinoma [53]. Cell survival, proliferation, and protein synthesis are regulated by the PI3K/AKT/mTOR pathway [54–56]. Stimulation of the PI3K/AKT/mTOR pathway has been linked to tumor development and reduced patient survival [57]. Recent studies on PI3K/AKT inhibitors suggest that recruiting the PI3K/AKT pathway is a potential strategy for treating breast cancer [58]. In humans, there are three primary MAPK pathways, but the pathway concerning ERK1/2 is the most relevant to breast cancer [59]. Genes involved in the ERK1/2 pathway directly regulate various fundamental biological functions, including differentiation, apoptosis, cellular proliferation, and survival [60]. Dysregulation of the MAPK/ERK cascade is a hallmark of robust carcinogenesis and several components of this pathway are mutated or exhibit aberrant expression in breast cancer [61,62]. To further elucidate the molecular mechanism behind the inhibitory action of the CA-4 analogue on malignant breast cancer, we investigated whether the CA-4 analogue modulates the PI3K/AKT and MAPK/ERK signaling pathways. Treatment with the CA-4 analogue resulted in the suppression of the PI3K/AKT and MAPK/ERK pathways, as evidenced by the reduction in phosphorylation levels of PI3K, AKT, MEK1/2, and ERK1/2 in breast cancer cells. Notably, the suppressive effect of CA-4 analogue on the PI3K/AKT and MAPK/ERK signaling was greater than that of CA-4 parent drug.

Moreover, several studies have revealed that the PI3K/AKT and MAPK/ERK cascades may interloop with each other and exhibit a synergistic effect in driving breast cancer proliferation [63,64]. Taken together, the CA-4 analogue could be a more potent anticancer drug against malignant breast cancer cells by simultaneously targeting the PI3K/AKT/mTOR and MAPK pathways [63,65].

5. Conclusions

The current research revealed that the CA-4 analogue exhibited superior suppression of cell proliferation compared to the parent CA-4 in breast cancer cells, such as hormonal-dependent breast cancer (MCF-7), HER-2 enriched breast cancer (MDA-MB453), and triple-negative breast cancer (MDA-MB231). The enhanced antiproliferative activity of the CA-4 analogue may be attributed to its ability to induce apoptosis and effectively inhibit two key signaling cascades, namely PI3K/AKT and MAPK/ERK, which play critical roles in chemoresistance and treatment failure. Overall, the CA-4 analogue can be considered a possible anticancer agent for the management of numerous genetic breast cancer types.

Availability of Data and Materials

The datasets used and/or analyzed during the current study are available from the corresponding author on reasonable request.

Author Contributions

DHA, MHN and MF conceived the idea and designed the research study. OMA and MAE performed the conceptualization. DHA, MHN and MF performed the research. OMA, MHN, MF and MAE provided help and advice on data analysis. MM, DHA, MHN, AAKE and MF analyzed the data. DHA, MHN, AAKE and MF wrote the manuscript. All authors contributed to editorial changes in the manuscript. All authors read and approved the final manuscript.

Ethics Approval and Consent to Participate

Not applicable.

Acknowledgment

Not applicable.

Funding

The current work was supported by Princess Nourah bint Abdulrahman University Researchers Supporting Project number (PNURSP2023R91), Princess Nourah bint Abdulrahman University, Riyadh, Saudi Arabia.

Conflict of Interest

The authors declare no conflict of interest.

Supplementary Material

Supplementary material associated with this article can be found, in the online version, at https://doi.org/10.31083/j.fbl2808185.

References

[1] WHO. Breast cancer. 2021. Available at: https://www.who.int/news-room/fact-sheets/detail/breast-cancer (Accessed: 12 July 2023).

[2] Fang X, Cao J, Shen A. Advances in anti-breast cancer drugs and the application of nano-drug delivery systems in breast cancer therapy. Journal of Drug Delivery Science and Technology. 2020; 57: 101662.

[3] Onitilo AA, Engel JM, Greenlee RT, Mukesh BN. Breast Cancer Subtypes Based on ER/PR and her2 Expression: Comparison of Clinicopathologic Features and Survival. Clinical Medicine & Research. 2009; 7: 4–13.

[4] Parvathaneni V, Chilamakuri R, Kulkarni NS, Baig NF, Agarwal S, Gupta V. Exploring Amodiaquine's Repurposing Potential in Breast Cancer Treatment-Assessment of In-Vitro Efficacy & Mechanism of Action. International Journal of Molecular Sciences. 2022; 23: 11455.

[5] Dai X, Cheng H, Bai Z, Li J. Breast Cancer Cell Line Classification and its Relevance with Breast Tumor Subtyping. Journal of Cancer. 2017; 8: 3131–3141.

[6] Tong CWS, Wu M, Cho WCS, To KKW. Recent Advances in the Treatment of Breast Cancer. Frontiers in Oncology. 2018; 8: 227.

[7] Kuo MT. Roles of Multidrug Resistance Genes in Breast Cancer Chemoresistance. Advances in Experimental Medicine and Biology. 2007; 608: 23–30.

[8] Nedeljković M, Damjanović A. Mechanisms of chemotherapy resistance in triple-negative breast cancer—how we can rise to the challenge. Cells. 2019; 8: 957.

[9] Bukowski K, Kciuk M, Kontek R. Mechanisms of multidrug resistance in cancer chemotherapy. International journal of molecular sciences. 2020; 21: 3233.

[10] Abdel-Hamid NM, Fathy M, Koike C, Yoshida T, Okabe M, Zho K, *et al*. Identification of Chemo and Radio-Resistant Sub-Population of Stem Cells in Human Cervical Cancer HeLa Cells. Cancer Investigation. 2021; 39: 661–674.

[11] Jana D, Zhao Y. Strategies for enhancing cancer chemodynamic therapy performance. Exploration. 2022; 2: 20210238.

[12] Miricescu D, Totan A, Stanescu-Spinu I-I, Badoiu SC, Stefani C, Greabu M. PI3K/AKT/mTOR signaling pathway in breast cancer: from molecular landscape to clinical aspects. International Journal of Molecular Sciences. 2020; 22: 173.

[13] Lim HN, Baek SB, Jung HJ. Bee venom and its peptide component melittin suppress growth and migration of melanoma cells via inhibition of PI3K/AKT/mTOR and MAPK pathways. Molecules. 2019; 24: 929.

[14] Nazmy M, Abu-baih D, El-Rehany M, Fathy M. Pathways of triple negative breast cancer. Minia Journal of Medical Research. 2021; 32: 1–3.

[15] Fathy M, Fawzy MA, Hintzsche H, Nikaido T, Dandekar T, Othman EM. Eugenol exerts apoptotic effect and modulates the sensitivity of HeLa cells to cisplatin and radiation. Molecules. 2019; 24: 3979.

[16] Fathy M, Sun S, Zhao QL, Abdel-Aziz M, Abuo-Rahma GEA, Awale S, *et al*. A New Ciprofloxacin-derivative Inhibits Proliferation and Suppresses the Migration Ability of HeLa Cells. Anticancer Research. 2020; 40: 5025–5033.

[17] Fawzy MA, Beshay ON, Bekhit AA, Abdel-Hafez SMN, Batiha GE, Bin Jardan YA, *et al*. Nephroprotective effect of at-MSCs against cisplatin-induced EMT is improved by azilsartan via attenuating oxidative stress and TGF-β/Smad signaling. Biomedicine & Pharmacotherapy. 2023; 158: 114097.

[18] Ramadan MF, Durazzo A, Lucarini M. Advances in Research on Food Bioactive Molecules and Health. Molecules. 2021; 26: 7678.

[19] Karatoprak GŞ, Küpeli Akkol E, Genç Y, Bardakci H, Yücel Ç, Sobarzo-Sánchez E. Combretastatins: an overview of structure, probable mechanisms of action and potential applications. Molecules. 2020; 25: 2560.

[20] Mustafa M, Abdelhamid D, Abdelhafez EMN, Ibrahim MAA, Gamal-Eldeen AM, Aly OM. Synthesis, antiproliferative, anti-tubulin activity, and docking study of new 1,2,4-triazoles as potential combretastatin analogues. European Journal of Medicinal Chemistry. 2017; 141: 293–305.

[21] Tron GC, Pirali T, Sorba G, Pagliai F, Busacca S, Genazzani AA. Medicinal Chemistry of Combretastatin a4: Present and Future Directions. Journal of Medicinal Chemistry. 2006; 49: 3033–3044.

[22] Carr M, Greene LM, Knox AJS, Lloyd DG, Zisterer DM, Meegan MJ. Lead identification of conformationally restricted β-lactam type combretastatin analogues: Synthesis, antiproliferative activity and tubulin targeting effects. European Journal of Medicinal Chemistry. 2010; 45: 5752–5766.

[23] Parihar S, Kumar A, Chaturvedi AK, Sachan NK, Luqman S, Changkija B, *et al*. Synthesis of combretastatin a4 analogues on steroidal framework and their anti-breast cancer activity. The Journal of Steroid Biochemistry and Molecular Biology. 2013; 137: 332–344.

[24] Mustafa M, Anwar S, Elgamal F, Ahmed ER, Aly OM. Potent combretastatin a-4 analogs containing 1,2,4-triazole: Synthesis, antiproliferative, anti-tubulin activity, and docking study. European Journal of Medicinal Chemistry. 2019; 183: 111697.

[25] Amin AH, Sharifi LMA, Kakhharov AJ, Opulencia MJC, Alsaikhan F, Bokov DO, *et al*. Role of Acute Myeloid Leukemia (AML)-Derived exosomes in tumor progression and survival. Biomedicine & Pharmacotherapy. 2022; 150: 113009.

[26] Mosmann T. Rapid colorimetric assay for cellular growth and survival: Application to proliferation and cytotoxicity assays. Journal of Immunological Methods. 1983; 65: 55–63.

[27] Mohammed HA, Abd El-Wahab MF, Shaheen U, Mohammed AE-SI, Abdalla AN, Ragab EA. Isolation, characterization, complete structural assignment, and anticancer activities of the methoxylated flavonoids from rhamnus disperma roots. Molecules. 2021; 26: 5827.

[28] Cornelissen M, Philippé J, De Sitter S, De Ridder L. Annexin V expression in apoptotic peripheral blood lymphocytes: an electron microscopic evaluation. Apoptosis. 2002; 7: 41–47.

[29] Mustafa M, Abuo-Rahma GEA, Abd El-Hafeez AA, Ahmed ER, Abdelhamid D, Ghosh P, *et al*. Discovery of antiproliferative and anti-FAK inhibitory activity of 1,2,4-triazole derivatives containing acetamido carboxylic acid skeleton. Bioorganic & Medicinal Chemistry Letters. 2021; 40: 127965.

[30] Abdel-Rahman IM, Mustafa M, Mohamed SA, Yahia R, Abdel-Aziz M, Abuo-Rahma GEA, *et al*. Novel Mannich bases of ciprofloxacin with improved physicochemical properties, antibacterial, anticancer activities and caspase-3 mediated apoptosis. Bioorganic Chemistry. 2021; 107: 104629.

[31] Mustafa M, Abd El-Hafeez AA, Abdelhamid D, Katkar GD, Mostafa YA, Ghosh P, *et al*. A first-in-class anticancer dual HDAC2/FAK inhibitors bearing hydroxamates/benzamides capped by pyridinyl-1,2,4-triazoles. European Journal of Medicinal Chemistry. 2021; 222: 113569.

[32] Hummon AB, Lim SR, Difilippantonio MJ, Ried T. Isolation and solubilization of proteins after TRIzol extraction of RNA and DNA from patient material following prolonged storage. Biotechniques. 2007; 42: 467–470, 472.

[33] Boesenberg-Smith KA, Pessarakli MM, Wolk DM. Assessment of DNA Yield and Purity: an Overlooked Detail of PCR Troubleshooting. Clinical Microbiology Newsletter. 2012; 34: 1–6.
[34] Almasmoum H. Characterization of mucin 2 expression in colorectal cancer with and without chemotherapies, in vivo and in vitro study. Journal of Umm Al-Qura University for Medical Sciences. 2021; 7: 18–22.
[35] Longo MC, Berninger MS, Hartley JL. Use of uracil DNA glycosylase to control carry-over contamination in polymerase chain reactions. Gene. 1990; 93: 125–128.
[36] Livak KJ, Schmittgen TD. Analysis of Relative Gene Expression Data Using Real-Time Quantitative PCR and the 2^{-CT} Method. Methods. 2001; 25: 402–408.
[37] Burnette WN. "Western blotting": electrophoretic transfer of proteins from sodium dodecyl sulfate–polyacrylamide gels to unmodified nitrocellulose and radiographic detection with antibody and radioiodinated protein A. Analytical Biochemistry. 1981; 112: 195–203.
[38] Stamos J, Sliwkowski MX, Eigenbrot C. Structure of the Epidermal Growth Factor Receptor Kinase Domain alone and in Complex with a 4-Anilinoquinazoline Inhibitor. Journal of Biological Chemistry. 2002; 277: 46265–46272.
[39] Brancato V, Gioiella F, Imparato G, Guarnieri D, Urciuolo F, Netti PA. 3D breast cancer microtissue reveals the role of tumor microenvironment on the transport and efficacy of free-doxorubicin in vitro. Acta Biomaterialia. 2018; 75: 200–212.
[40] Veldwijk MR, Neumaier C, Gerhardt A, Giordano FA, Sütterlin M, Herskind C, *et al*. Comparison of the proliferative and clonogenic growth capacity of wound fluid from breast cancer patients treated with and without intraoperative radiotherapy. Translational Cancer Research. 2015; 4: 173–177.
[41] Ueno NT, Zhang D. Targeting EGFR in Triple Negative Breast Cancer. Journal of Cancer. 2011; 2: 324–328.
[42] Ishikawa T, Ichikawa Y, Shimizu D, Sasaki T, Tanabe M, Chishima T, *et al*. The role of HER-2 in Breast Cancer. Journal of Surgery and Science. 2014; 2: 4–9.
[43] Peng F, Liao M, Qin R, Zhu S, Peng C, Fu L, *et al*. Regulated cell death (RCD) in cancer: key pathways and targeted therapies. Signal Transduction and Targeted Therapy. 2022; 7: 286.
[44] Pistritto G, Trisciuoglio D, Ceci C, Garufi A, D'Orazi G. Apoptosis as anticancer mechanism: function and dysfunction of its modulators and targeted therapeutic strategies. Aging. 2016; 8: 603–619.
[45] Qian S, Wei Z, Yang W, Huang J, Yang Y, Wang J. The role of BCL-2 family proteins in regulating apoptosis and cancer therapy. Frontiers in Oncology. 2022; 12: 985363.
[46] Lin K, Rong Y, Chen D, Zhao Z, Bo H, Qiao A, *et al*. Combination of ruthenium complex and doxorubicin synergistically inhibits cancer cell growth by down-regulating PI3K/AKT signaling pathway. Frontiers in Oncology. 2020; 10: 141.
[47] Guo XZ, Shao XD, Liu MP, Xu JH, Ren LN, Zhao JJ, *et al*. Effect of bax, bcl-2 and bcl-xL on regulating apoptosis in tissues of normal liver and hepatocellular carcinoma. World Journal of Gastroenterology. 2002; 8: 1059–1062.
[48] Naseri MH, Mahdavi M, Davoodi J, Tackallou SH, Goudarzvand M, Neishabouri SH. Up regulation of Bax and down regulation of Bcl2 during 3-NC mediated apoptosis in human cancer cells. Cancer Cell International. 2015; 15: 55.
[49] Aubrey BJ, Kelly GL, Janic A, Herold MJ, Strasser A. How does p53 induce apoptosis and how does this relate to p53-mediated tumour suppression? Cell Death & Differentiation. 2018; 25: 104–113.
[50] Bai L, Wang S. Targeting Apoptosis Pathways for New Cancer Therapeutics. Annual Review of Medicine. 2014; 65: 139–155.
[51] Cai G, Wang Y, Houda T, Yang C, Wang L, Gu M, *et al*. MicroRNA-181a suppresses norethisterone-promoted tumorigenesis of breast epithelial MCF10A cells through the PGRMC1/EGFR-PI3K/Akt/mTOR signaling pathway. Translational Oncology. 2021; 14: 101068.
[52] Jeong Y, Bae SY, You D, Jung SP, Choi HJ, Kim I, *et al*. EGFR is a therapeutic target in hormone receptor-positive breast cancer. Cell Physiol Biochem. 2019; 53: 805-819.
[53] Kamal A, Lakshma Nayak V, Nagesh N, Vishnuvardhan MVPS, Subba Reddy NV. Benzo[b]furan derivatives induces apoptosis by targeting the PI3K/Akt/mTOR signaling pathway in human breast cancer cells. Bioorganic Chemistry. 2016; 66: 124–131.
[54] Franke TF, Hornik CP, Segev L, Shostak GA, Sugimoto C. PI3K/Akt and apoptosis: size matters. Oncogene. 2003; 22: 8983–8998.
[55] Alaaeldin R, Hassan HA, Abdel-Rahman IM, Mohyeldin RH, Youssef N, Allam AE, *et al*. A New EGFR Inhibitor from Ficus benghalensis Exerted Potential Anti-Inflammatory Activity via Akt/PI3K Pathway Inhibition. Current Issues in Molecular Biology. 2022; 44: 2967–2981.
[56] Fawzy MA, Maher SA, El-Rehany MA, Welson NN, Albezrah NKA, Batiha GE-S, *et al*. Vincamine Modulates the Effect of Pantoprazole in Renal Ischemia/Reperfusion Injury by Attenuating MAPK and Apoptosis Signaling Pathways. Molecules. 2022; 27: 1383.
[57] Zheng W, Cao L, Ouyang L, Zhang Q, Duan B, Zhou W, *et al*. Anticancer activity of 1,25-$(OH)_2D_3$ against human breast cancer cell lines by targeting Ras/MEK/ERK pathway. OncoTargets and Therapy. 2019; 12: 721–732.
[58] Gonzalez-Angulo AM, Blumenschein GR. Defining biomarkers to predict sensitivity to PI3K/Akt/mTOR pathway inhibitors in breast cancer. Cancer Treatment Reviews. 2013; 39: 313–320.
[59] Yin X, Zhang J, Li X, Liu D, Feng C, Liang R, *et al*. DADS suppresses human esophageal xenograft tumors through RAF/MEK/ERK and mitochondria-dependent pathways. International Journal of Molecular Sciences. 2014; 15: 12422–12441.
[60] Lin Z, Zhang C, Zhang M, Xu D, Fang Y, Zhou Z, *et al*. Targeting cadherin-17 inactivates Ras/Raf/MEK/ERK signaling and inhibits cell proliferation in gastric cancer. PLoS ONE. 2014; 9: e85296.
[61] Peng J, Gassama-Diagne A. Apicobasal polarity and Ras/Raf/MEK/ERK signalling in cancer. Gut. 2017; 66: 986–987.
[62] Wan L, Chen M, Cao J, Dai X, Yin Q, Zhang J, *et al*. The APC/C E3 Ligase Complex Activator FZR1 Restricts BRAF Oncogenic Function. Cancer Discovery. 2017; 7: 424–441.
[63] Shimizu T, Tolcher AW, Papadopoulos KP, Beeram M, Rasco DW, Smith LS, *et al*. The Clinical Effect of the Dual-Targeting Strategy Involving PI3K/AKT/mTOR and RAS/MEK/ERK Pathways in Patients with Advanced Cancer. Clinical Cancer Research. 2012; 18: 2316–2325.
[64] Wang Y, Nie H, Zhao X, Qin Y, Gong X. Bicyclol induces cell cycle arrest and autophagy in HepG2 human hepatocellular carcinoma cells through the PI3K/AKT and Ras/Raf/MEK/ERK pathways. BMC Cancer. 2016; 16: 742.
[65] Saini KS, Loi S, de Azambuja E, Metzger-Filho O, Saini ML, Ignatiadis M, *et al*. Targeting the PI3K/AKT/mTOR and Raf/MEK/ERK pathways in the treatment of breast cancer. Cancer Treatment Reviews. 2013; 39: 935–946.